A Study of Finite Hydrodynamic Slider Bearings

Lubricated With Ferro fluids

Gamal Shafik Nada*

Department of Mechanical Engineering, Higher Technological Institute, Tenth of Ramadan City, Egypt

* Corresponding author.
E-mail: Gamalnada@hti.edu.eg

Abstract: An effort has been made to study and analyze the performance of a finite hydrodynamic slider bearing lubricated by Ferro fluid. The modified Reynolds' equation, pressure differential equation, that contains the magnetic effect of the ferro-lubricant is derived and solved numerically and the results of the overall static characteristics namely; pressures, load-carrying capacity, pressure center, friction force and friction coefficient are determined and presented in this study. Also, the flow rates in the bearing are evaluated. The study indicates that the wedge parameter has an optimum value (about 1.25) which gives higher load capacity, lower friction force and lower friction coefficient. Also, the width to length ratio has an important role in the performance of finite bearings until value equal 4, while the wider bearing has non-significant effect on the performance. It is also shown that the magnetic effect of the ferro-lubricant has significant improving effect on the overall static characteristics of the slider bearing.

Keywords: Finite-slider Bearing, Hydrodynamic Lubrication, Ferrofluid Lubricant, Static Characteristics

LIST OF SYMBOLS

a difference between the inlet and outlet film thickness, m

B bearing width, m

B_m magnetic field density vector, $T = Wb/m^2$

E_o relative difference required for stopping the iteration process $= 10^{-12}$

F_m magnetic force vector per unit volume, N/m^3

F_{mx} magnetic force component in x direction, N/m^3

F_{mz} magnetic force component in z direction, N/m^3

F friction force at the slider surface, N

F^* non-dimensional friction force $F^* = \frac{F h_o}{\mu U L B}$

h film thickness, m

h_i film thickness at the bearing inlet, m

h_o film thickness at the bearing outlet, m

h^* non-dimensional film thickness $h^* = h/h_o$

H_m magnetic field vector, A/m

h_m magnetic field intensity, A/m

h_{mc} characteristic value of the magnetic field intensity $= I/2\pi L$, A/m

h_m^* non-dimensional magnetic field intensity $h_m^* = \frac{h_m}{h_{mc}} = \frac{h_m}{I/2\pi L}$

k normal distance from the wire to the bearing surface, m

k^* non-dimensional distance from the wire to the bearing surface $k^* = k/L$

L bearing length, m

I current intensity passing through the wire, A

M magnetization of the ferrofluid, A/m

p lubricant pressure, pa

p_i inlet pressure to the bearing, pa

p_o outlet pressure from the bearing, pa

p^* non-dimensional pressure $p^* = \frac{p h_o^2}{\mu U L}$

Q_x flow rate in x direction, m^3/s

Q_x^*	non-dimensional flow rate in x direction	$Q_x^* = \frac{2Q_x}{BUh_o}$
Q_{xo}^*	non-dimensional flow rate in x direction at the bearing outlet (at x^*=1), m^3/s	
Q_z	flow rate in z direction, m^3/s	
Q_z^*	non-dimensional flow rate in z direction	$Q_z^* = \frac{2Q_z}{BUh_o}$
Q_{zo}^*	non-dimensional flow rate in z direction at one end of the bearing (at $z^* = 0$ or $z^* = 1$)	
r	distance from the wire to any point on the bearing, m	
U	sliding velocity, m/s	
V	velocity vector, m/s	
u, v, w	velocity component in x, y, and z directions, m/s	
W	load carrying capacity, N	
W^*	non-dimensional load carrying capacity	
X_m	susceptibility of the ferro-fluid, dimensionless	
x, y, z	Cartesian coordinates	
x^*	non-dimensional coordinate in x direction	$x^* = x/L$
Δx^*	non-dimensional increment in x^* direction	
x_p^*	non-dimensional pressure center coordinate in x direction	
z^*	non-dimensional coordinate in z direction	$z^* = z/B$
Δz^*	non-dimensional increment in z^* direction	
z_p^*	non-dimensional pressure center coordinate in z direction	
$\propto$	wedge parameter $\alpha = \frac{a}{h_o}$, dimensionless	
β	width to length ratio $\beta = B/L$, dimensionless	
γ	magnetic force coefficient $\gamma = \frac{\mu_o X_m h_{mc}^2 h_o^2}{\mu UL}$, dimensionless	
ρ	fluid density, kg/m^3	
μ	fluid viscosity coefficient $pa. s$	
μ_o	permeability of free space $= 4\pi \times 10^{-7}\ N/A^2$	
τ	sheer stress, pa	

1. INTRODUCTION

The most important property of magnetic fluids is that they can be made to adhere to any desired surface with the aid of magnets. When a magnetic field is applied, each particle experiences magnetic body force which causes it to move. When all the particles start moving, they cause the colloidal homogeneous suspension to move en masse, one of the novel ferrofluid lubricant is superparamagnetic nano-lubricants [1]. Owing to these features, ferro-fluids are useful in many applications [2-3].   In the field of lubrication, Chang et al [4], Zhang [5] and Urreta et al [6] made studies of the characteristics of magnetized journal bearing lubricated with ferrofluid. Their results indicated that high bearing performance was obtained compared with the ordinary fluid lubrication. A novel ferrofluid bearing with controllable damping effect is designed by Liu et al [7]. Their results show that this type of bearing with variable damping is useful in a wide range of control systems.

In slider bearings: Das [8] presented a theoretical study of slider bearings in the presence of a uniform magnetic field. Ochon´ski [9] presented some new designs of sliding bearings lubricated with ferrofluids. These designs gave advantages over conventional ball bearings. Patel et al [10] made study and analysis about the performance of a magnetic fluid based infinitely short slider bearing. Expression of the load-carrying capacity for infinitely wide bearing was introduced under thermal effects by Singh et al [11]. Shah and Patel [12] performed a study of magnetic fluid lubrication of porous pivoted slider bearing with slip and squeeze velocity. Patel et al made studies on the performance of a ferrofluid lubrication of rough porous slider bearings with different configurations [13-16]. They found that the magnetization decreases the negative effects caused by the roughness or slip velocity. The same results were obtained by Shukla and Deheri [17]. Patel and Dehere [18] made an investigation of thin film lubrication at nanoscale for a ferrofluid infinitely long slider bearing.

These researches used assumption of infinitely short or infinitely long bearing (one-dimensional bearing). Also, they applied theoretical magnetic field models in dealing with the ferrofluid lubrication. In this work, more realistic magnetic field model was applied on finite slider bearing (two-dimensional) with wide range of width to length ratios. In this model, the magnetic field is produced by carrying-current infinitely long wire. The magnetic field strength and then the obtained magnetic force can be easily controlled by changing the position of the wire with respect to the bearing and also by changing the intensity of the electric current passing through it. This model was used previously in the study of the hydrodynamic journal bearings [19]. This work studies its effect on the slider bearings.

2.ANALYSIS

The configuration of the slider bearing is displayed in Fig. 1. The expression for the film thickness h between the slider and the bearing is given by:
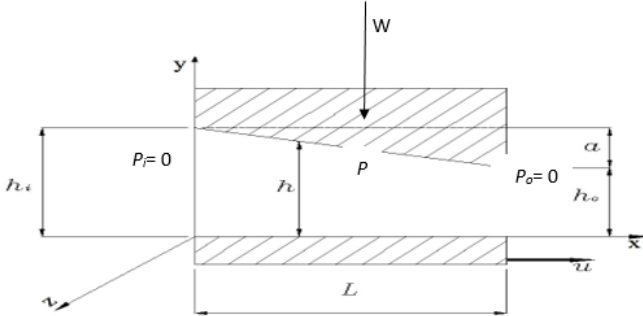

Fig 1. Geometry of a slider

$$h = h_o + a\ (1 - x/L) \tag{1}$$

In dimensionless form:

$$h^* = 1 + \propto (1 - x^*) \tag{2}$$

Where: $\propto = a/h_o$ (wedge parameter of the bearing)

The equations of motion and continuity of the fluid lubricant will be:

$$\rho \frac{dV}{dt} = -\nabla p + \mu \nabla^2 V + F_m \tag{3}$$

$$\nabla \cdot V = 0 \tag{4}$$

By neglecting the inertia force term $\rho \frac{dV}{dt}$ and using the usual assumptions of hydrodynamic lubrication applicable to thin films [20], the equations in Cartesian coordinates are reduced to:

$$\frac{\partial p}{\partial x} = \mu \frac{\partial^2 u}{\partial y^2} + F_{mx} \tag{5}$$

$$\frac{\partial p}{\partial z} = \mu \frac{\partial^2 w}{\partial y^2} + F_{mz} \tag{6}$$

$$\frac{\partial p}{\partial y} = 0 \tag{7}$$

$$\frac{\partial u}{\partial x} + \frac{\partial v}{\partial y} + \frac{\partial w}{\partial z} = 0 \tag{8}$$

The boundary conditions are: $u = U$, $w = 0$ (at $y = 0$) and $u = 0$, $w = 0$ (at $y = h$). Integrations of Equation (5) then Equation (6) using the above boundary conditions, the velocities in x and z directions are obtained.

$$u = (1 - y/h)U + \frac{1}{2\mu}\left(\frac{\partial p}{\partial x} - F_{mx}\right) \cdot (y^2 - yh) \tag{9}$$

$$w = \frac{1}{2\mu}\left(\frac{\partial p}{\partial z} - F_{mz}\right) \cdot (y^2 - yh) \tag{10}$$

Substituting about these velocities in Equation (8) and integration across the film thickness, the modified Reynolds' equation is obtained.

$$\frac{\partial}{\partial x}\left(h^3 \frac{\partial p}{\partial x}\right) + \frac{\partial}{\partial z}\left(h^3 \frac{\partial p}{\partial z}\right) = 6\mu U\left(\frac{\partial h}{\partial x}\right) + \frac{\partial}{\partial x}(h^3 F_{mx}) + \frac{\partial}{\partial z}(h^3 F_{mz}) \tag{11}$$

The magnetic force is calculated by [21]:

$$F_m = curl\ H_m \times B_m + \mu_o M \cdot grad\ H_m \tag{12}$$

For non-conductive fluid, the induced free current ($curl\ H_m$) equals zero and the magnetic force F_m and its components in x and z direction become:

$$F_m = \mu_o M\ \nabla H_m = \mu_o X_m h_m\ \nabla H_m, \text{ and}$$

$$F_{mx} = \mu_o X_m h_m\ (\partial h_m/\partial x) \tag{13}$$

$$F_{mz} = \mu_o X_m h_m\ (\partial h_m/\partial z) \tag{14}$$

Substituting about these magnetic force components into Equation (11), the modified Reynolds' becomes:

$$\frac{\partial}{\partial x}\left(h^3 \frac{\partial p}{\partial x}\right) + \frac{\partial}{\partial z}\left(h^3 \frac{\partial p}{\partial z}\right) = 6\mu U\left(\frac{\partial h}{\partial x}\right) +$$

$$\mu_o X_m \frac{\partial}{\partial x}\left(h^3 h_m \frac{\partial h_m}{\partial x}\right) + \mu_o X_m \frac{\partial}{\partial z}\left(h^3 h_m \frac{\partial h_m}{\partial z}\right) \tag{15}$$

in dimensionless form:

$$\frac{\partial}{\partial x^*}\left(h^{*3} \frac{\partial p^*}{\partial x^*}\right) + \frac{1}{\beta^2}\frac{\partial}{\partial z^*}\left(h^{*3} \frac{\partial p^*}{\partial z^*}\right) = 6\frac{\partial h^*}{\partial x^*} +$$

$$\gamma \frac{\partial}{\partial x^*}\left(h^{*3} h_m^* \frac{\partial h_m^*}{\partial x^*}\right) + \frac{\gamma}{\beta^2}\frac{\partial}{\partial z^*}\left(h^{*3} h_m^* \frac{\partial h_m^*}{\partial z^*}\right) \tag{16}$$

The used magnetic field model, Fig. 2., is produced by infinitely long carrying-current wire. The wire is placed at the middle (at $x = L/2$) parallel to the bearing width and at a distance k from the bearing surface. The magnetic field distribution around the wire are concentric circles of radius r with center lies on the wire. The magnetic field intensity is then given by:
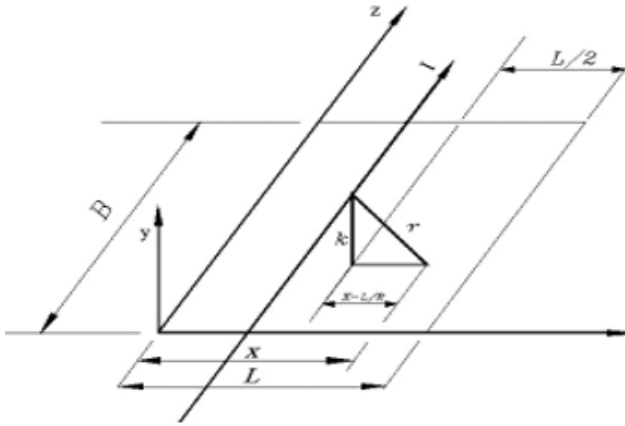
FIG 2. The magnetic field model, concentric infinitely long carrying-current wire displaced distance k from the bearing surface

$$h_m = I/2\pi r = I/2\pi(k^2 + (x - L/2)^2)^{1/2}$$

(17)

In dimensionless form:

$$h_m^* = 1/\left(k^{*2} + (x^* - 0.5)^2\right)^{1/2}$$ (18)

Where: $k^* = k/L$, k^* was chosen to be 0.25. This magnetic field has no gradient

in z direction, then, equation (16) is

reduced to:

$$\frac{\partial}{\partial x^*}\left(h^{*3}\frac{\partial p^*}{\partial x^*}\right) + \frac{1}{\beta^2}\frac{\partial}{\partial z^*}\left(h^{*3}\frac{\partial p^*}{\partial z^*}\right) = 6\frac{\partial h^*}{\partial x^*} + \gamma\frac{\partial}{\partial x^*}\left(h^{*3} h_m^* \frac{\partial h_m^*}{\partial x^*}\right)$$

(19)

3.NUMERICAL CALCULATIONS

Equation (19) is solved numerically by finite difference technique using boundary conditions for the film pressure as:

$p^* = 0$ at $x^* = 0$, $z^* = 0$ (zero inlet atmospheric pressure p_i) and $p^* = 0$ at $x^* = 1$, $z^* = 1$ (zero outlet atmospheric pressure p_o). By Applying the central difference approximation for derivatives, equation (19) can be written as:

$$A_o p_{i,j}^* = A_1 p_{i-1,j}^* + A_2 p_{i+1,j}^* + A_3 p_{i,j-1}^* + A_4 p_{i,j+1}^* + A_5$$

(20)

Where:

$$A_1(i,j) = \frac{h_{i,j}^{*3}}{\Delta x^{*2}} - 3h_{i,j}^{*2}\left(\frac{h_{i+1,j}^* - h_{i-1,j}^*}{4\Delta x^{*2}}\right) \qquad A_2(i,j) = \frac{h_{i,j}^{*3}}{\Delta x^{*2}} + 3h_{i,j}^{*2}\left(\frac{h_{i+1,j}^* - h_{i-1,j}^*}{4\Delta x^{*2}}\right)$$

$$A_3(i,j) = \frac{h_{i,j}^{*3}}{\beta^2 \Delta z^{*2}} - 3h_{i,j}^{*2}\left(\frac{h_{i,j+1}^* - h_{i,j-1}^*}{4\beta^2 \Delta z^{*2}}\right)$$

$$A_4(i,j) = \frac{h_{i,j}^{*3}}{\beta^2 \Delta z^{*2}} + 3h_{i,j}^{*2}\left(\frac{h_{i,j+1}^* - h_{i,j-1}^*}{4\beta^2 \Delta z^{*2}}\right)$$

$$A_o(i,j) = 2h_{i,j}^{*3}\left(\frac{1}{\Delta x^{*2}} + \frac{1}{\beta^2 \Delta z^{*2}}\right)$$

$$A_5(i,j) = -6\frac{h_{i+1,j}^* - h_{i-1,j}^*}{2\Delta x^*} -$$

$$\gamma h_{i,j}^{*3}\left(h_{mi,j}^*\left(\frac{h_{mi+1,j}^* - 2h_{mi,j}^* + h_{mi-1,j}^*}{\Delta x^{*2}}\right) + \left(\frac{h_{i+1,j}^* - h_{i-1,j}^*}{2\Delta x^*}\right)^2 + h_{mi,j}^*\left(\frac{h_{mi,j+1}^* - 2h_{mi,j}^* + h_{mj-1}^*}{\beta^2 \Delta z^{*2}}\right) + \left(\frac{h_{mi,j+1}^* - h_{mj-1}^*}{2\beta \Delta z^*}\right)^2\right)$$

$$-3\gamma h_{i,j}^{*2} h_{mi,j}^*\left(\frac{h_{i+1,j}^* - h_{i-1,j}^*}{2\Delta x^*}\right)\left(\frac{h_{mi+1,j}^* - h_{mi-1,j}^*}{2\Delta x^*}\right) 3\gamma h_{i,j}^{*2} h_{mi,j}^*$$

$$\left(\frac{h_{i,j+1}^* - h_{i,j-1}^*}{2\beta \Delta z^*}\right)\left(\frac{h_{mi,j+1}^* - h_{mi,j-1}^*}{2\beta \Delta z^*}\right)$$

The field of solution is divided into 51 sections in the x∗ direction and 51 sections in the z∗ direction ($\Delta z^* = \Delta x^* = 0.02$). This is after some trials to choose the grid size which doesn't affect on the accuracy of results. By Guass-Siedel iteration process:

$$p_{i,j}^{*n} = (A_1 p_{i-1,j}^{*n} + A_2 p_{i+1,j}^{*n-1} + A_3 p_{i,j-1}^{*n} + A_4 p_{i,j+1}^{*n-1} + A_5)/A_o$$

(21)

Where n is the iteration number. By assuming initial pressure distribution and using Eq. (21), the new pressure distribution is yielded. The iterative procedure will continue and the results converge until it finally stops when the relative difference in pressure distribution between two successive iterations falls below $E_o = 10^{-12}$,

$E_o = \frac{\sum_{i=1,j=1}^{i=N,j=M}|p_{i,j}^{*n} - p_{i,j}^{*n-1}|}{\sum_{i=1,j=1}^{i=N,j=M}|p_{i,j}^{*n}|}$. From the obtained pressure distribution, the bearing characteristics will be determined as follow:

- The load carrying capacity is given by:

$$W^* = W\left(\frac{h_o^2}{\mu U L^2 B}\right) = \int_{x^*=0}^{x^*=1}\int_{z^*=0}^{z^*=1} p^* dx^* dz^* = \sum_{I=1}^{i=N}\sum_{j=1}^{j=M} p_{i,j}^* \Delta x^* \Delta z^*$$

(22)

- The pressure center or the point of action of W^* is given by:

$$x_p^* = \frac{x_p}{L} = \frac{\int_{x^*=0}^{x^*=1}\int_{z^*=0}^{z^*=1} p^* x^* dx^* dz^*}{\int_{x^*=0}^{x^*=1}\int_{z^*=0}^{z^*=1} p^* dx^* dz^*} = \frac{\sum_{I=1}^{i=N}\sum_{j=1}^{j=M} p_{i,j}^* x_{i,j}^* \Delta x^* \Delta z^*}{\sum_{I=1}^{i=N}\sum_{j=1}^{j=M} p_{i,j}^* \Delta x^* \Delta z^*}$$

(23)

$$z_p^* = \frac{z_p}{L} = \frac{\int_{x^*=0}^{x^*=1}\int_{z^*=0}^{z^*=1} p^* z^* dx^* dz^*}{\int_{x^*=0}^{x^*=1}\int_{z^*=0}^{z^*=1} p^* dx^* dz^*} = \frac{\sum_{I=1}^{i=N}\sum_{j=1}^{j=M} p_{i,j}^* z_{i,j}^* \Delta x^* \Delta z^*}{\sum_{I=1}^{i=N}\sum_{j=1}^{j=M} p_{i,j}^* \Delta x^* \Delta z^*}$$

(24)

- The friction force at the slider surface is given by:

$$F = \int_{x=0}^{x=L}\int_{z=0}^{z=B} [\tau]_{y=0} \, dx dz = \int_{x=0}^{x=L}\int_{z=0}^{z=B} \left[\mu \frac{\partial u}{\partial y}\right]_{y=0} dx dz$$

(25)

Using equation (9) to determine $\frac{\partial u}{\partial y}$, the friction force can be written as:

$$F = \int_{x=0}^{x=L}\int_{z=0}^{z=B} \left[(\frac{\partial p}{\partial x} - F_{mx})(y - h/2) - \mu U/h\right]_{y=0} dx dz$$

(26)

Substituting about F_{mx} from equation (13),

$$F = \int_{x=0}^{x=L}\int_{z=0}^{z=B} \left[(\frac{\partial p}{\partial x} - \mu_o X_m h_m \frac{\partial h_m}{\partial x})(y - h/2) - \right.$$
$$\left. \mu U/h\right]_{y=0} dx dz \quad (27)$$

In dimensionless form, the friction force at the slider (at $y=0$) is given by:

$$F^* = \frac{F h_o}{\mu U L B} = \int_{x^*=0}^{x^*=0}\int_{z^*=0}^{z^*=1} \left[\frac{h^*}{2}(\frac{\partial p^*}{\partial x^*} - \gamma h_m^* \frac{\partial h_m^*}{\partial x^*}) + \right.$$
$$\left. \frac{1}{h^*}\right] dx^* dz^* = \sum_{I=1}^{i=N}\sum_{j=1}^{j=M} \left[\frac{h_{i,j}^*}{2}(\frac{p_{i+1,j}^* - p_{i-1,j}^*}{2\Delta x^*}) - \right.$$
$$\left. \gamma h_{mi,j}^*(\frac{h_{mi+1,j}^* - h_{mi-1,j}^*}{2\Delta x^*}) + \frac{1}{h_{i,j}^*}\right] \Delta x^* \Delta z^* \quad (28)$$

- The friction coefficient is given by $\frac{F}{W} = (\frac{h_o}{L}) \frac{F^*}{W^*}$, then the modified friction coefficient is given by:

$$f = \frac{F^*}{W^*} = (\frac{L}{h_o}) \frac{F}{W}$$

(29)

- The flow rate in x direction is given by:

$$Q_x = \int_{z=0}^{z=B}\int_{y=0}^{y=h} u \, dy dz$$

(30)

Using equation (9) then equation (13) and by integrating across the film thickness:

$$Q_x = \int_{z=0}^{z=B} \left[-\frac{h^3}{6} \cdot \frac{1}{2\mu}(\frac{\partial p}{\partial x} - \mu_o X_m h_m \frac{\partial h_m}{\partial x}) + \frac{Uh}{2}\right] dz$$

(31)

In dimensionless form:

$$Q_x^* = \frac{2Q_x}{B U h_o} = \int_{z^*=0}^{z^*=1} \left[-\frac{h^{*3}}{6}(\frac{\partial p^*}{\partial x^*} - \gamma h_m^* \frac{\partial h_m^*}{\partial x^*}) + h^*\right] dz^* =$$
$$\sum_{j=1}^{j=M} \left[-\frac{h_{i,j}^{*3}}{6}(\frac{p_{i+1,j}^* - p_{i-,j}^*}{2\Delta x^*}) - \gamma h_{mi,j}^*(\frac{h_{mi+1,j}^* - h_{mi-1,j}^*}{2\Delta x^*}) + h_{i,j}^*\right] \Delta z^*$$

(32)

- The flow rate in z direction is given by:

$$Q_z = \int_{x=0}^{x=L}\int_{y=0}^{y=h} w \, dy dx$$

(33)

Using equation (10) then equation (14) and by integrating across the film thickness:

$$Q_z = \int_{x=0}^{x=L} \left[-\frac{h^3}{6}\frac{1}{2\mu}(\frac{\partial p}{\partial z} - \mu_o X_m h_m \frac{\partial h_m}{\partial z})\right] dx$$

(34)

In dimensionless form:

$$Q_z^* = \frac{2Q_z}{B U h_o} = \int_{x^*=0}^{x^*=1} \left[-\frac{h^{*3}}{6\beta^2}(\frac{\partial p^*}{\partial z^*} - \gamma h_m^* \frac{\partial h_m^*}{\partial z^*})\right] dx^*$$

(35)

The magnetic field has $\frac{\partial h_m^*}{\partial z^*} = 0$, then

$$Q_z^* = \int_{x^*=0}^{x^*=1} \left[-\frac{h^{*3}}{6\beta^2}(\frac{\partial p^*}{\partial z^*})\right] dx^* = \sum_{i=1}^{i=N} \left[-\frac{h_{i,j}^{*3}}{6\beta^2}(\frac{p_{i,j+1}^* - p_{i,j-1}^*}{2\Delta z^*})\right] \Delta x^*$$

(36)

4. RESULTS AND DISCUSSION

The accuracy of the present model is firstly verified by comparing the obtained pressure distribution, for □=0, and also the load capacity with the results in the literature [20]. The comparison indicates that there is agreement between them. The modified Reynolds equation, equation (19), indicates that the slider bearing performance depends on geometrical parameters (wedge parameter ∝ and width to length ratio β) and magnetic parameter (magnetic force coefficient γ). This equation was solved numerically using the following values:

- Wedge parameter ∝ from 0.25 up to 3, these values cover wide range of the wedge effect.
- Width to length ratio β from 0.5 (short bearing) to 10 (very wide bearing).
- Magnetic force coefficient γ□□= 0 (no magnetic effect), 0.05 (moderate magnetic effect) and 0.1 (high magnetic effect), [19].

Effect of the above parameters on the bearing performance is discussed.

Figure 3 shows the pressure distribution, at the middle section of the bearing, versus the distance x^* along the bearing length. As shown, the pressure increases with the increase of magnetic force coefficient γ. The maximum pressure is doubled when $\gamma = 0.05$ and becomes very high at $\gamma = 0.1$ with shifting its position to $x^*=0.5$ where the carrying-current wire is placed. The magnetic effect at this region is very intense.
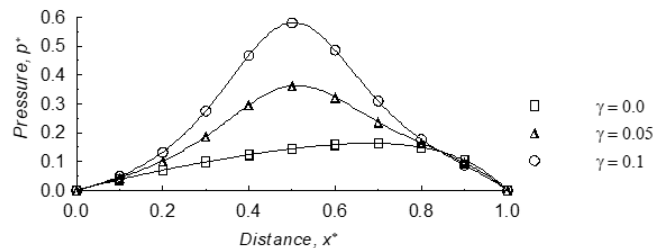

Fig3. Variation of the pressure p^* at the middle section of the bearing, with the distance x^* with respect to magnetic force coefficient γ, $\beta = 1$, ∝= 1

The results of the pressure distributions are reflected on the static characteristics of the bearing. The results of the load-carrying capacity are shown in Figs. 4-5. The load capacity increases with the increase of $\propto$ □up to nearly 1.25), Fig. 4. With further increase of $\propto$, the load capacity becomes unchanged and some decrease occurs at the higher values. These results are attributed to the increase of the pressure as a result of increase of the wedge action with the increase of $\propto$, while at high values of it there is a corresponding increase of the film thickness which leads to the decrease of the pressure. Figure 5 shows that the load capacity

increases with high rates by the increase of β up to value equals 4. For the wider bearings, there is a little or neglected increase. The magnetic effect is obviously shown in the two figures where there is large increase of the load capacity with
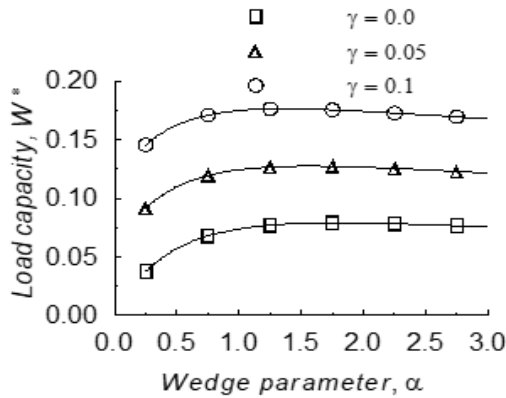
the increase of the magnetic force coefficient γ.
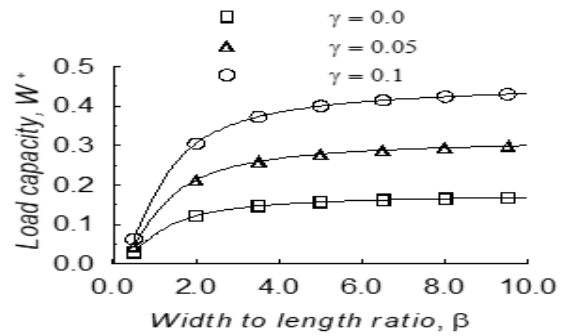
Fig 4. Variation of W^* with respect to $\propto$ and γ, $\beta=1$

Fig 5. Variation of W^* with respect to β and γ, $\propto=1$

The bearing and the magnetic field are symmetric about middle of the bearing width. The results of the pressure center confirm this symmetry where $z_p^* = 0.5$. As shown, for non-magnetic fluid, Table 1, the position of the pressure center is shifted towards the bearing outlet (increase of x_p^*) with the increase of $\propto$, where the film thickness is small and the hydrodynamic effect is high. For magnetic lubricant, Table 2, the pressure center become nearer to the middle of the bearing ($x_p^* \cong 0.5$) where the carrying-current wire is positioned and the magnetic effect is very high. Effect of width to length ratio β on the pressure center is also shown.

TABLE 1. The pressure center, x^*_p, z^*_p for different values of the wedge parameter $\propto$ and width to length ratio β for non-magnetic bearing, $\gamma = 0.0$

	$\beta = 1$			$\propto= 1$		
	$\propto$	x_p^*	z_p^*	β	x_p^*	z_p^*
	0.25	0.53	0.5	0.5	0.6	0.5
	0.5	0.54	0.5	1	0.57	0.5
	1	0.57	0.5	1.5	0.56	0.5
	1.5	0.59	0.5	2	0.56	0.5
	2	0.6	0.5	4	0.56	0.5
$\gamma = 0$	2.5	0.62	0.5	8	0.55	0.5
	3	0.63	0.5	10	0.55	0.5

TABLE 2. The pressure center, x^*_p, z^*_p for different values of the wedge parameter $\propto$ and width to length ratio β for magnetic bearing with $\gamma = 0.1$

	$\beta = 1$			$\propto = 1$		
	$\propto$	x^*_p	z^*_p	β	x^*_p	z^*_p
	0.25	0.5	0.5	0.5	0.5	0.5
	0.5	0.5	0.5	1	0.51	0.5
	1	0.51	0.5	1.5	0.52	0.5
$\gamma = 0.1$	1.5	0.52	0.5	2	0.52	0.5
	2	0.53	0.5	4	0.52	0.5
	2.5	0.53	0.5	8	0.52	0.5
	3	0.53	0.5	10	0.52	0.5

Figure 6 shows inverse effect of the wedge parameter $\propto$ on the friction force. Also, there is a pronounced reduction of the friction force with the increase of the magnetic force coefficient γ. Equation (28) shows how the magnetic effect causes decrease of the shear stress and then the friction force at the slider surface. Figure 7 certifies the decreasing effect of the magnetic force coefficient on the friction force. It also shows how the increase of the width to length ratio causes increase of the friction force until β reaches nearly 4. Then, the wider bearings have not significant effect on the friction force.
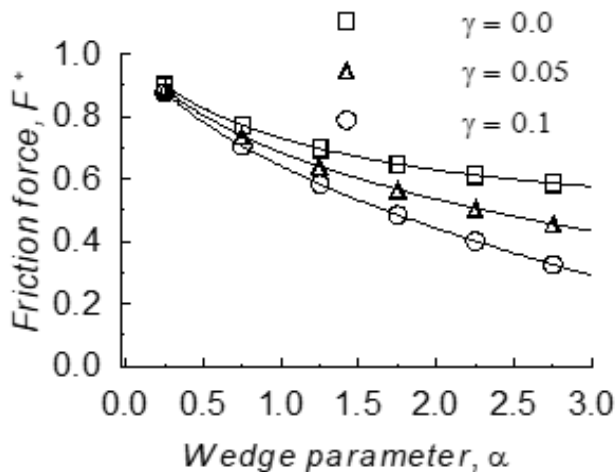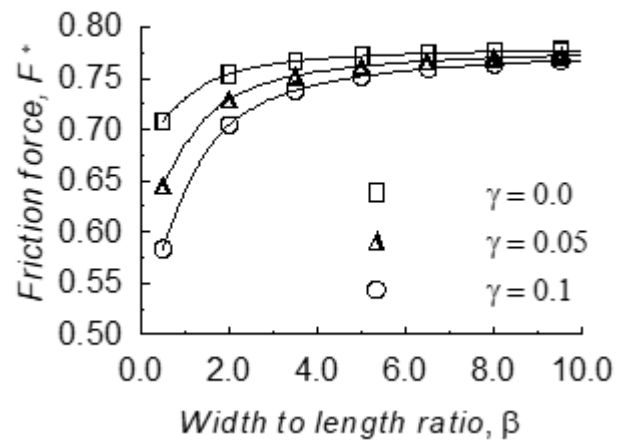

Fig 7. Variation of F^* with respect to β and γ, $\propto=1$

The results of the friction coefficient are shown in Figs. 8-9. There is large decrease of the friction coefficient with the increase of $\propto$ for its low and moderate values, and some little decrease for the higher values. Increase of β causes decrease of the friction coefficient until it nearly equals 4. For the wider bearings, the friction coefficient is nearly unchanged. The two figures show the decrease of the friction coefficient with the increase of the magnetic effect.
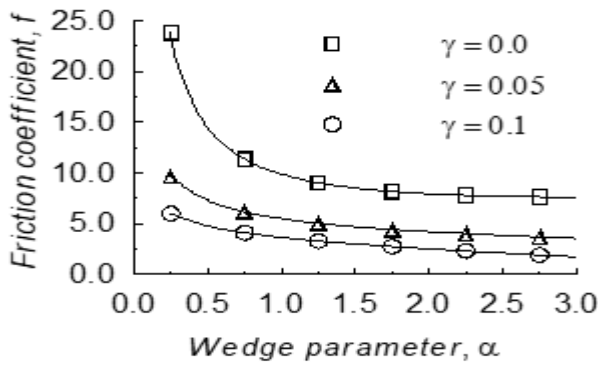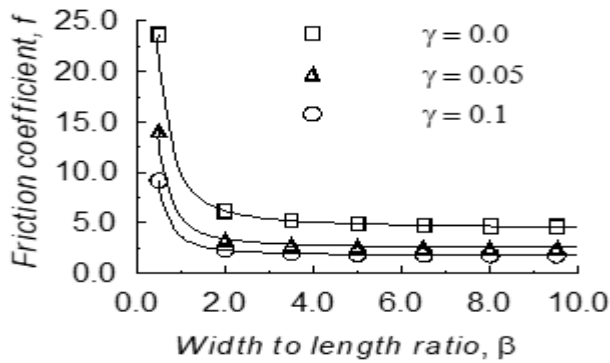

Fig 6. Variation of F^* with respect to $\propto$ and γ, $\beta=1$

Fig 8. Variation of f with respect to $\propto$ and γ, β=1

Fig 9. Variation of f with respect to β and γ, $\propto$=1

Figures 10-11 show the effect of wedge parameter and width to length ratio on the flow rate in x direction at the bearing outlet. There is some increase of the flow rate with the increase of $\propto$ or β. The increase becomes insignificant for the wide bearing. The two figures show that the magnetic field has some sealing effect where the flow rate decreases with the increase of the magnetic force coefficient γ. Equation (32) indicates how the sealing effect is obtained by the magnetic field that has a gradient in x direction
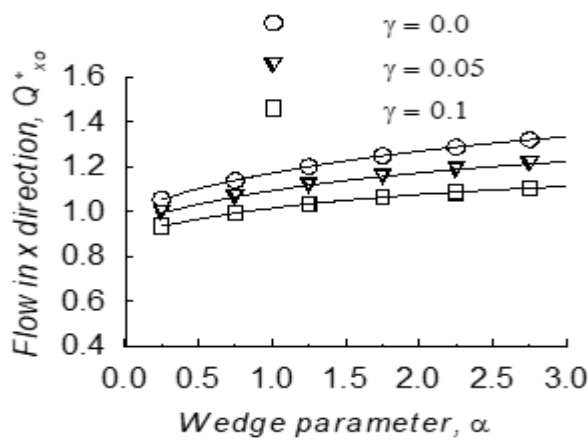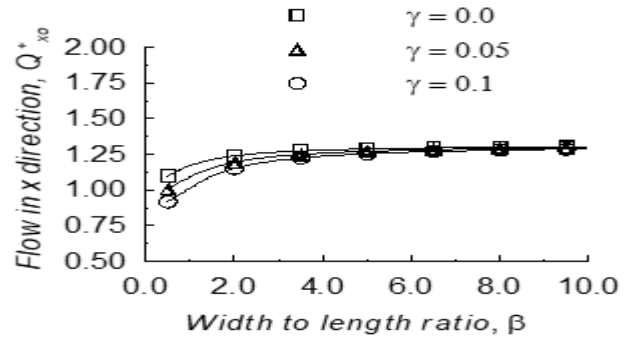

Fig 10. variation of Q_{xo}^* with respect to $\propto$ and γ, β=1

Fig 11. Variation of Q_{xo}^* with respect to β and γ, $\propto$=1

Figure 12 shows the effect of $\propto$ on the side flow at one end of the bearing (at $z^* = 0$ or $z^* = 1$). The flow rate in z direction increases with the increase of wedge parameter $\propto$. Increase of $\propto$ causes increase of the film thickness for the same value of h_o. These result in increase of the area the lubricant flow through it. The used magnetic field model has no field gradient in z direction. So, the magnetic effect has no sealing effect on the side flow. Effect of width to length ratio β on the side flow is shown in Fig. 13. Increasing of β causes decrease of the side flow. Increasing of the bearing width, results in decrease of the pressure gradient along the bearing width. Infinitely wide bearing means $\partial p^*/\partial z^* = 0$ and nearly zero leakage was obtained, equation (36).

The used magnetic field model is the field produced by a carrying-current wire displaced distance k from the bearing surface, Fig. 2. Effect of the non-dimensional distance k^* on the bearing performance is given in Fig. 14. Increasing the distance of the wire from the bearing surface causes decrease of the magnetic field intensity that reaches the bearing. The decrease of the magnetic effect results in decrease of the load-carrying capacity, increasing of the friction force and friction coefficient. At high values of k^* (more than 1), the magnetic effect becomes insignificant and the change in the bearing performance is neglected. The presented results were obtained with $k^* = 0.25$
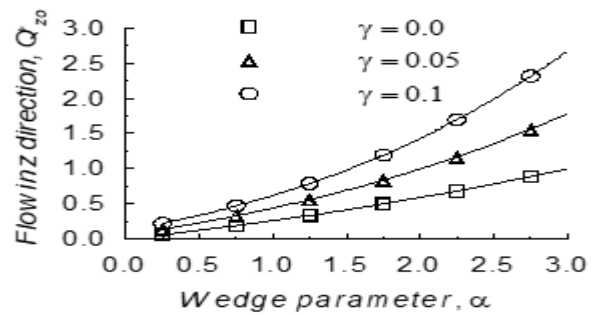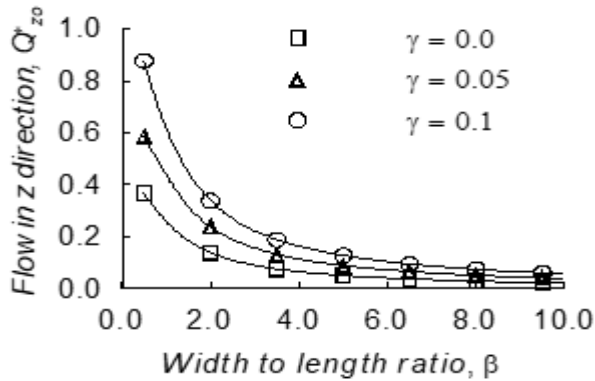

Fig 12. Variation of Q_{zo}^* with respect to $\propto$ and γ, β=1

Fig 13. Variation of Q_{zo}^* with respect to β and γ, $\propto=1$
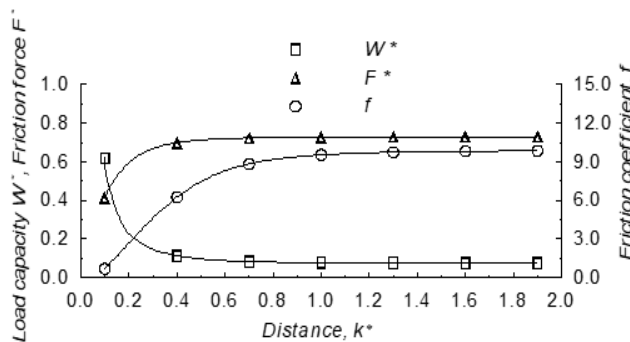

Fig 14. Effect of the distance of the wire from the bearing surface k^* on the load capacity W^*, friction force F^* and friction coefficient f, $\propto=1$, $\beta=1$ and $\gamma=0.1$

5 CONCLUSION

The Slider bearing characteristics; namely, the load-carrying capacity, the friction force, the friction coefficient and the flow rates depend on the wedge parameter for both magnetic and non-magnetic lubricant. The optimum value of the wedge parameter that gives maximum load capacity is about 1.25.

The width to length ratio plays an important role on the slider bearing performance even there are magnetic effects or not. Increasing the width to length ratio gives high load capacity, it increases 3 times for wide bearing compared with short bearing for non-magnetic bearing and increases 5 times for magnetic bearing. Also, it causes high frictional force but with low friction coefficient. The flow rate Q_x is increased while the side flow Q_z is highly decreased (It becomes ¼ for wide bearing compared to its value for short bearing). These effects are for aspect ratio up to 4. The wider bearing has non-significant effect.

The magnetic force coefficient has improving significant effect on the performance of the slider bearing for all values of its geometrical parameters. Increasing the magnetic force coefficient leads to increase of the load-carrying capacity (It increases nearly 3 times compared with non-magnetic bearing) with pressure center becomes nearer to the middle of the bearing, decrease of the friction

force and decrease of the friction coefficient (it becomes nearly ¼ of its value for non-magnetic bearing). The used magnetic field model has some sealing effect for the flow in x direction. As the magnetic coefficient, $\gamma = \frac{\mu_o X_m h_{mc}^2 h_o^2}{\mu U L}$, changes inversely with the velocity U and directly with the square film thickness h_o, the ferrofluid lubricant is more suitable for low and moderate velocities and also at large film thickness.

REFERENCES

[1] A. E. D. S. Guedes, V. S. Mello, F. Bohn & S. M. Alves "Understanding the Influence of the Magnetic Field, Particle Size, and Concentration on the Tribological Performance of Superparananolubricants" Tribology Transactions, 64, 2021, pp 551-561.

[2] M. Goldowsky, "New Methods for Sealing, Filtering, and Lubricating with Magnetic Fluids", *IEEE Transactions on Magnetics* 16, 1980, pp. 382-386.

[3] J. S. Gorla, K. Ramalingam and I. Adluri, "Magnetohydrodynamic Breaking", *ASME Journal of Tribology* 117, 1995, pp. 724-728.

[4] H. S. Chang, C. Q. Chi, and P.Z. Zhao, "A Theoretical and Experimental Study of Ferrofluid Lubricated Four-Pocket Journal Bearings", *Journal of Magnetism and Magnetic Materials* 65, 1987, pp. 372-374.

[5] Y. Zhang, "Static Characteristics of Magnetized Journal Bearing Lubricated with Ferrofluid", *ASME Journal of Tribology* 113, 1991, pp. 533-538.

[6] H. Urreta, Z. Leicht, A. Sanchez, A. Agirre, P. Kuzhir and G. Magnac, "Hydrodynamic Bearing Lubricated with Magnetic Fluids", *Journal of Physics*, 149, 2009, pp. 1-4.

[7] X. Liu, L. Sun, Z. Fang, H. Hu, J. Zhen, C. Chen, Y. Wu and M. h. Hajiyan "Vibration Characteristics of Controllable Damping Ferrofluid Bearing" Tribology Transactions, 63, 2020, pp. 55-65

[8] N.C. Das, "A Study of Optimum Load-Carrying Capacity for Slider Bearings Lubricated with Couple Stress Fluids in Magnetic Field", *Tribology international* 31, 1998, pp. 393-400.

[9] W. Ochon´ski, "Sliding Bearing Lubricated with Magnetic Fluids", *Industrial lubrication and technology* 59, 2007, pp. 252-265.

[10] R. M. Patel, G. M. Deheri and P. A.Vadher, "Performance of a Magnetic Fluid-based Short Bearing", *Acta polytechnica hungarica* 7, 2010, pp. 63-78.

[11] J. P. Singh, and N. Ahmad, "Analysis of a Porous-Inclined Slider Bearing Lubricated with Magnetic Fluid Considering Thermal Effects with Slip Velocity", *J. of the Braz. Soc. of Mech. Sci. & Eng.* 33, 2011, pp. 351-356.

[12] R. C. Shah, and D. B. Patel, "Magnetic Fluid Lubrication of Porous Pivoted Slider Bearing with Slip and Squeeze Velocity", *Int. J. Industrial Mathematics*, 6, 2014, pp. 199-206.

[13] S. J. Patel, G.M. Deheri, J. R. and Patel, "Ferrofluid Lubrication of a Rough Porous Hyperbolic Slider Bearing with Slip Velocity", *Tribology in Industry* 36, 2014, pp. 259-268.

[14] S. J. Patel, G.M. Deheri, and J. R. Patel, "Shliomis Model Based Ferrofluid Lubrication of a Rough Porous Convex Pad Slider Bearing", *Tribology in Industry*, 38, 2016, pp. 57-65.

[15] S. J. Patel, G.M. Deheri, and J. R Patel, "Ferrofluid Lubrication of a Rough Porous Secant-Shaped Slider Bearing with Slip Velocity", *Journal of the Serbian Society for Computational Mechanics* 11 No.1, 2017, pp. 69-81.

[16] S. J. Patel, G.M. Deheri, and J. R. Patel, "Mathematical Model of Shliomis Model Based Ferrofluid Lubricated Porous Convex Pad

Slider Bearing with Effect of Slip Velocity", *International Journal of Applied Mathematics & Statistical Sciences* 9, 2020, pp. 39-48.

[17] S. Shukla, and G. Deheri, "Ferro Fluid Based Rough Porous Tilted Pad Bearing with Slip Effect", *International Conference on Research and Innovations in Science, Engineering &Technology* 1, 2017, pp. 134–140.

[18] J. R. Patel, and G.M. Deheri, "A Study of Thin Film Lubrication at Nanoscale for A Ferrofluid Based Infinitely Long Rough Porous Slider Bearing", *Series: Mechanical Engineering* 14, No. 1, 2016, pp. 89-99.

[19] G. S. Nada, T. A. Osman, and Z. S. Safar, "Effect of Using Carrying-Current Wire Models in The Design of Hydrodynamic Journal Bearings Lubricated with Ferro-Fluid", *Tribology Letters* 11 No. 1, 2001, pp. 61-70.

[20] B. J. Hamrock, "Fundamentals of Fluid Film Lubrication", McGraw-Hill, Inc. New York, 1994.

[21] R. E. Zelazo, and J. R. Melcher, "Dynamic and Stability of Ferrofluids: Surface Interaction", *Journal of Fluid Mech.* 39, 1969, pp. 1-24.